THE JOURNAL OF BIOLOGICAL CHEMISTRY VOL. 288, NO. 20, pp. 13951–13959, May 17, 2013

Investigation of *in Vivo* Roles of the C-terminal Tails of the Small Subunit ($\beta\beta'$) of *Saccharomyces cerevisiae* Ribonucleotide Reductase

CONTRIBUTION TO COFACTOR FORMATION AND INTERSUBUNIT ASSOCIATION WITHIN THE ACTIVE HOLOENZYME[*] [◆]

Received for publication, March 5, 2013, and in revised form, March 24, 2013 Published, JBC Papers in Press, March 25, 2013, DOI 10.1074/jbc.M113.467001

Yan Zhang[‡], **Xiuxiang An**[§], **JoAnne Stubbe**[‡¶], **and Mingxia Huang**[§1]

From the Departments of [‡]*Chemistry and* [¶]*Biology, Massachusetts Institute of Technology, Cambridge, Massachusetts 02139 and the* [§]*Department of Biochemistry and Molecular Genetics, University of Colorado School of Medicine, Aurora, Colorado 80045*

Background: *S. cerevisiae* ribonucleotide reductase (RNR) comprises α and $\beta\beta'$ subunits in an $(\alpha_2)_m(\beta\beta')_n$ active holoenzyme.
Results: C-terminal tail mutants of $\beta\beta'$ prevent radical transfer across the α-β interface and consequently deoxynucleotide production *in vivo*.
Conclusion: The $\beta\beta'$ C-terminal tails interact only with the proximal α within each $\alpha/\beta(\alpha/\beta')$ pair.
Significance: The predisposition of the $\beta\beta'$ C-terminal tails in active RNR *in vivo* is established.

The small subunit (β_2) of class Ia ribonucleotide reductase (RNR) houses a diferric tyrosyl cofactor (Fe^{III}_2-$Y^{\bullet}$) that initiates nucleotide reduction in the large subunit (α_2) via a long range radical transfer (RT) pathway in the holo-$(\alpha_2)_m(\beta_2)_n$ complex. The C-terminal tails of β_2 are predominantly responsible for interaction with α_2, with a conserved tyrosine residue in the tail (Tyr^{356} in *Escherichia coli* NrdB) proposed to participate in cofactor assembly/maintenance and in RT. In the absence of structure of any holo-RNR, the role of the β tail in cluster assembly/maintenance and its predisposition within the holo-complex have remained unknown. In this study, we have taken advantage of the unusual heterodimeric nature of the *Saccharomyces cerevisiae* RNR small subunit ($\beta\beta'$), of which only β contains a cofactor, to address both of these issues. We demonstrate that neither β-Tyr^{376} nor β'-Tyr^{323} (Tyr^{356} equivalent in NrdB) is required for cofactor assembly *in vivo*, in contrast to the previously proposed mechanism for *E. coli* cofactor maintenance and assembly *in vitro*. Furthermore, studies with reconstituted-$\beta\beta'$ and an *in vivo* viability assay show that β-Tyr^{376} is essential for RT, whereas Tyr^{323} in β' is not. Although the C-terminal tail of β' is dispensable for cofactor formation and RT, it is essential for interactions with β and α to form the active holo-RNR. Together the results provide the first evidence of a directed orientation of the β and β' C-terminal tails relative to α within the holoenzyme consistent with a docking model of the two subunits and argue against RT across the β β' interface.

Ribonucleotide reductase (RNR)[2] catalyzes the reduction of nucleoside 5′-diphosphates to the corresponding deoxynucleotides in all organisms (1, 2). The class Ia RNRs are composed of α and β subunits. In *Escherichia coli*, the active quaternary structure is $\alpha_2\beta_2$ (3, 4), whereas in eukaryotic RNRs including *Saccharomyces cerevisiae*, the active structure is likely $\alpha_2\beta_2$ and/or $(\alpha_2)_3\beta_2$ and $(\alpha_2)_3(\beta_2)_3$ (5–9). α_2 contains the active site where nucleoside 5′-diphosphates are reduced and the allosteric effector binding sites that control which substrate is reduced and the rate of the overall reduction (1, 10). β_2 houses a diferric tyrosyl radical cofactor (Fe^{III}_2-$Y^{\bullet}$) assembled from Fe^{II}, O_2, and a reducing equivalent into the active Fe^{III}_2-$Y^{\bullet}$ cofactor ($\sim$1 $Y^{\bullet}/\beta_2$) that is essential to nucleotide reduction. During each turnover, the $Y^{\bullet}$ in β_2 oxidizes a cysteine in the active site of α_2 that is 35 Å removed from the β metal center β_2 (see Fig. 1), which initiates nucleotide reduction (11).

Atomic resolution structures of *E. coli* α_2 and of β_2 from the Eklund group (12, 13) led them to propose a docking model for the active $\alpha_2\beta_2$ complex, which in conjunction with biochemical studies (14–18) demonstrated the importance of the C-terminal tail of each β (15 and 8 amino acids in the prokaryotic and eukaryotic RNRs, respectively) for the interaction with α. Although their model had the tail from each β associated with the corresponding α, an equally probable model could have the tail of β associated with the adjacent α (see Fig. 2, *right panel*). Unfortunately, the C termini (30–35 amino acids) of all β_2 structures are disordered (19), and thus, the molecular details of the tail with respect to both itself and α remain unknown.

Within this C-terminal tail resides a conserved tyrosine residue, Tyr^{356} in *E. coli* β_2, that has been proposed to play an important role in electron transfer in Fe^{III}_2-$Y^{\bullet}$ cluster assembly from both the Fe^{II}_2 and the Fe^{III}_2 (met) state in β_2 (1) and in the long range RT to initiate nucleotide reduction in α_2 (see Figs. 1*A* and Fig. 2, *left* and *center panels*). In the former case, efforts to regenerate $Y^{\bullet}$ from the met state of the cofactor using a

* This work was supported, in whole or in part, by National Institutes of Health Grants GM29595 (to J. S.), CA125574 (to M. H.), and GM81393 (to J. S. and M. H.).
◆ This article was selected as a Paper of the Week.
[1] To whom correspondence should be addressed. Tel.: 303-724-3204; E-mail: mingxia.huang@ucdenver.edu.
[2] The abbreviations used are: RNR, ribonucleotide reductase; α_2, ribonucleotide reductase large subunit; β_2, $\beta\beta'$ ribonucleotide reductase small subunit homodimer and heterodimer; Fe^{III}_2-$Y^{\bullet}$, diferric tyrosyl radical; RT, radical transfer; CSM, complete supplemental mixture(s); 5-FOA, 5-fluoroorotic acid; aa, amino acids.

TABLE 1
Yeast strains used in this study

Strains	Genotype	Parental Strain
Y300	*MATa can1–100 ade2–1 his3–11,15 leu2–3,112 trp1-, ura3–1*	Y300
MHY593	*MATa rnr2::KanMX6, pMH881 (URA3CENRNR2)*	Y300
MHY20	*MATa rnr4::LEU2, pMH140 (URA3CENRNR4)*	Y300
RNR2-WT shuffle	*MATa rnr2::KanMX6, pMH881 (URA3CENRNR2)* pMH811 (pRS314-P_{RNR2}-3xMyc-RNR2)	Y300
AXY853	*MATa rnr2::KanMX6, pMH881 (URA3CENRNR2)* pMH1669 (pRS314-P_{RNR2}-3xMyc-rnr2 (Y376F))	Y300
RNR4-WT shuffle	*MATa rnr4::LEU2, pMH140 (URA3CENRNR4)*pMH569 (pRS413-P_{RNR4}-HA-RNR4)	Y300
AXY854	*MATa rnr4::LEU2, pMH140 (URA3CENRNR4)* pMH1668 (pRS413-P_{RNR4}-HA-rnr4 (Y323F))	Y300
BY4741	*MATa his3Δ1, leu2Δ0, met15Δ0, ura3Δ0*	BY4741
GalRNR2	*MATa rnr2::HisMX6-P_{GAL1}-RNR2*	BY4741
AXY1619	*MATa rnr2::HisMX6-P_{GAL1}-RNR2 pRS415*	BY4741
AXY1620	*MATa rnr2::HisMX6-P_{GAL1}-RNR2 pRS415*-P_{RNR2}-3xMyc-RNR2	BY4741
AXY1621	*MATa rnr2::HisMX6-P_{GAL1}-RNR2 pRS415*-P_{RNR2}-3xMyc-rnr2 (Y376F)	BY4741

Y356A mutant gave only low levels of Y• relative to the wild-type (WT) control. Thus, electron transfer required for reducing the Fe_2^{III} state was prohibited by this mutation. Deletion of the C-terminal tail also gave poor recovery of Y• in efforts to assemble the cofactor from the Fe_2^{II} state (20). In the latter case, recent studies using unnatural tyrosine analogs site-specifically in place of Tyr^{356} revealed that $Tyr^{356•}$ plays an essential role in Cys^{439} oxidation in α_2 (21) (see Fig. 1*A*).

The RNR of the budding yeast *S. cerevisiae* possesses several unique properties that have made it feasible to investigate the functions proposed for the C-terminal tail of β_2 and more specifically the conserved tyrosine residue (Tyr^{356}, see Fig. 1*B*) within the tail. In contrast with the small β_2 subunit of most organisms, the yeast small subunit is a heterodimer *in vivo*, $\beta\beta'$, encoded by the *RNR2* and *RNR4* genes, respectively (22–25). β' is structurally homologous to β but lacks three iron ligands, and as a consequence, contains no metallo-cofactor (18, 22, 25–27). Although β' is catalytically inactive, it is required for converting β into a conformation that is competent for iron loading and Y• formation *in vitro* and *in vivo* (23, 24, 28). Importantly, recombinant apo-β_2 and β'_2 rapidly form apo-$\beta\beta'$ *in vitro* (24), and although cluster assembly from Fe^{II}, O_2, and reductant is inefficient (0.25 Y•/$\beta\beta'$), these properties allow us to study reconstitution *in vitro* with mutant small subunits.

Although β is essential for cell viability, cells lacking β' (Δ*rnr4*) are viable, albeit with extremely low Y• content and RNR activity in some yeast strain backgrounds (*e.g.* S288C) (29). These strains are also hypersensitive to the Y• quenching reagent hydroxyurea (28). We have been able to take advantage of this viability and our ability to permeabilize WT and Δ*rnr4* cells to take up proteins (*e.g.* α,β') to provide a robust assay for *in vivo* Fe_2^{III}-Y• cofactor assembly by the addition of β'_2 and assay for RNR activity by the addition of β'_2 followed by α_2 (28) herein.

In this study, we have also used EPR spectroscopy on whole cells and permeabilized cells to show *in vivo* that the C-terminal 8 amino acids of β', rich in carboxylates, are not required for binding and delivery of iron to β and that consequently this tail does not function as a molecular chaperone as we originally proposed from *in vitro* studies (18). We also demonstrate that β-Tyr^{376} is not on an essential electron transfer pathway to deliver the reducing equivalent to generate the Fe_2^{III}-Y• cofactor from the Fe_2^{II} or met (Fe_2^{III} tyrosyl radical reduced) state either *in vitro* or *in vivo*. Moreover, studies using plasmid shuffle strains reveal that β-Tyr^{376} is nevertheless essential for the long range RT and cell survival, whereas β'-Tyr^{323} is not essential. Finally, although the β' mutant lacking the C-terminal 8 amino acids (β'-Δ8aa) is capable of heterodimer formation with β and supporting Fe_2^{III}-Y• cofactor assembly in β, the resulting $\beta\beta'$ is catalytically inactive (< 0.5% WT activity), suggesting an essential role of the β' tail for interactions with α_2 to form an active holo-enzyme. Our results for the first time provide *in vivo* evidence for the predisposition of the C-terminal tails of β and β' relative to α in the active RNR; these tails interact only with the α in the α/β (α/β') pair in the holo-RNR and do not cross over to interact with the adjacent α (see Fig. 2, *right panel*).

EXPERIMENTAL PROCEDURES

Strains, Plasmids, and Media—Yeast strains and plasmids used in this study are listed in Tables 1 and 2, respectively. Rich YPD medium contains 1% yeast extract, 2% peptone, and 2% glucose. Synthetic, defined 6.7 g/liter yeast nitrogen base without amino acids (Difco), 2% glucose, complete supplemental mixtures (CSM), or CSM with dropout of amino acid(s) (MP Biomedicals). Solid media contain 1.5% agar (Difco) as a solidifying agent. YP- and CSM-raffinose media contain 2% raffinose as the sole carbon source, which maintains the *GAL1* promoter at residual activity level (uninduced state). YP- and CSM-Raff/Gal media contain 2% raffinose and 0.5% galactose that activate the *GAL1* promoter (induced state).

Plasmids pMH813 (pRS415-P_{RNR2}-3×Myc-RNR2) and pMH569 (pRS413-P_{RNR4}-HA-RNR4) contain an N-terminal in-frame triple-Myc and HA epitope between the promoter and coding sequences of *RNR2* and *RNR4*, respectively (25). The *rnr2-Y376F* and *rnr4-Y323F* harboring plasmids pMH1669 and pMH1668 were constructed by using site-directed mutagenesis on pMH813 and pMH569 and were introduced into the plasmid shuffle strains MHY593 (*MATa*, *rnr2*::*KanMX6*, *pMH881 (URA3CENRNR2)*) and MHY20 (*rnr4*::*LEU2*, *pMH140 (URA3CENRNR4)*), respectively, as described (25).

The *GalRNR2* strain was constructed by replacing the endogenous promoter of *RNR2* with the *GAL1* promoter as described (28, 30) and maintained in YP-Raff/Gal medium. Plasmids pMH813 (RNR2) and pMH1669 (*rnr2-Y376F*), as well as the vector control pRS415, were introduced into the *GalRNR2* strain, and the transformants were selected and maintained on CSM-Leu Raff/Gal plates, resulting in AXY1619 (*GalRNR2 pRS415*), AXY1620 (*GalRNR2 pRS415-P_{RNR2}-3*×

TABLE 2
Plasmids used in this study

Plasmid	Features	Reference
pY1A	T7 promoter-driven yeast *RNR1* ORF	31
$p(His)_6$-Y2	T7 promoter-driven yeast *RNR2* ORF, N-terminal His_6 tag pET-14b vector	31
pHis-Y4	T7 promoter-driven yeast *RNR4* ORF, N-terminal His_6 tag pET-14b vector	31
pHis-Y4Δ	T7 promoter-driven yeast *RNR4* ORF, C-terminal 8 a.a. truncated, N-terminal His_6 tag, pET-14b vector	18
$p(His)_6$-Y2-Y376F	T7 promoter-driven yeast *RNR2* ORF, N-terminal His_6 tag pET-14b vector; site-directed mutagenesis Y376F introduced to $p(His)_6$-Y2	This study
pHis-Y4-Y323F	T7 promoter-driven yeast *RNR4* ORF, N-terminal His_6 tag pET-14b vector; site-directed mutagenesis Y323F introduced to pHis-Y4	This study
pMH813	*pRS415-P_{RNR2}-3xMyc-RNR2, CEN LEU2*	25
pMH1669	*pRS415-P_{RNR2}-3xMyc-rnr2 (Y376F), CEN LEU2*	This study
pMH569	*pRS413-P_{RNR4}-HA-RNR4, CEN HIS3*	25
pMH1668	*pRS413-P_{RNR4}-HA-rnr4 (Y323F), CEN HIS3*	This study

Myc-RNR2), and AXY1621(*GalRNR2 pRS415-P_{RNR2}-3×Myc-rnr2(Y376F)*) strains.

E. coli BL21 (DE3) cells transformed with previously constructed pET-14b vectors $p(His)_6$-RNR2 (β), pHis-RNR4 (β′), and pHis-RNR4Δ8aa (β′Δ8aa) (18) were used to express His_6-β, His_6-β′, and His_6-β′Δ8aa, respectively. Site-directed mutagenesis studies were performed using the QuikChange kit (Stratagene) to introduce Y376F and Y323F mutations into $p(His)_6$-β and $p(His)_6$-β′, respectively, and the changes were confirmed by sequencing. *E. coli* BL21 CodonPlus (DE3) RIL cells transformed with pY1A (31) were used to express α.

Purification of Recombinant α, His_6-β, His_6-β′, His_6-β′Δ8aa, His_6-β-Y376F, and His_6-β′-Y323F—E. coli transformants harboring the desired expression vectors were grown in LB medium with antibiotics (ampicillin or kanamycin) at 37 °C to an A_{600} of 0.4–0.8 before cooling the cultures to 16 °C by adjusting the temperature setting of the incubator. Induction of subunit expression was carried out by the addition of 0.5 mM (for β and β′) or 1 mM (for α) isopropyl β-D-1-thiogalactopyranoside to the medium, and growth was continued for 16 h. The proteins were purified as described previously (18, 24, 31). α was purified using a DEAE Sephadex column and a dATP affinity column (31) and had a specific activity of 102 nmol min^{-1} mg^{-1} when assayed in the presence of a 10× molar excess of FLAG-tagged ββ′ (specific activity 3000 nmol min^{-1} mg^{-1}) that was isolated from yeast Δ*crt1* MHY619 cells (29). Wild-type (WT) and mutant β and β′ were both N-terminally His_6-tagged with the following N terminus: MGSSHHHHHHSS-GLVPRGSH-native protein, and were purified by using an nickel-nitrilotriacetic acid column as described (18). All purified proteins were homogeneous as judged by SDS-PAGE.

Reconstitution of Fe^{III}_2-Y• Cofactor in ββ′—Reconstitution of Fe^{III}_2-Y• with β_2 and β'_2 was carried out using previously reported protocols (32). Briefly, purified β_2 and β'_2 were degassed on a Schlenk line and brought into an anaerobic box (MBraun) in a cold room. The β_2 and β'_2 were mixed for 2 min before the addition of 3 eq of ferrous iron. The resulting reaction mixture (137 μl) contained 44 μM each of β_2 and β'_2, 50 mM HEPES at pH 7.6, 5% glycerol and was incubated in the glove box for 10 min. The sample was then removed from the box, and 165 μl of O_2-saturated buffer was added and mixed immediately at room temperature, resulting in 20 μM ββ′. The sample (260 μl) was transferred to EPR tubes, and the rest of the sample was frozen immediately and used for subsequent activity assays.

Permeabilized Δrnr4 Yeast Cells Reconstituted with RNR4 and Analyzed by EPR Spectroscopy—A suspension of Δ*rnr4* cell (60 μl, 32 A_{600}/ml) permeabilized as described previously (28) was added to 200 μl of 0.1 M potassium P_i buffer (pH 7.5) containing 0.6 M sorbitol, 50 mM DTT, and 6.5 μM His_6-β'_2 or His_6-$(\beta'\Delta 8aa)_2$. The reaction mixture was incubated at 30 °C for 3 min before being transferred into an EPR tube and rapidly frozen in liquid nitrogen. Our previous study has found that rapid and efficient Fe^{III}_2-Y• cofactor assembly (0.5–0.6 Y•/ββ′ in contrast with 0.25–0.3 Y•/ββ′ *in vitro*) in permeabilized Δ*rnr4* cells requires high levels (50 mM) of DTT, although its specific role in the process is unclear (28).

EPR spectra were acquired on a Bruker EMX X-band spectrometer at 30 K using an Oxford Instruments liquid helium cryostat. Acquisition parameters for reconstitution in permeabilized cells and whole cell EPR with intact cells at 9.4 GHz were 0.2-milliwatt power, 1.8×10^5 gain, 2-G modulation amplitude, and 100-kHz modulation frequency. Spin quantitation was performed by double integration of the signal using *E. coli* NrdB as a standard in which the Y• concentration was determined by the dropline correction method (33). Analysis was carried out using WinEPR software (Bruker).

RNR Activity Assays—Activity of ββ′ in Δ*rnr4* permeabilized cells was measured as described previously (28). Typically, a solution (180 μl) containing 0.1 M potassium P_i, pH 7.5, 0.6 M sorbitol, 3 mM ATP, 10 mM NaF, 50 mM DTT, 4.4 μM α (specific activity 102 nmol min^{-1} mg^{-1}), and 7.7 μM His_6-β'_2 or His_6-$(\beta'\Delta 8aa)_2$ was mixed with 1.5 A_{600} Δ*rnr4* permeabilized cells (180 μl) at 4 °C and warmed at 30 °C for 1 min. The reaction was started by the addition of 1 mM [5-^{3}H]CDP (ViTrax, 17 Ci/mmol, 5790 cpm/nmol). Aliquots (58 μl) were removed at 0, 5, and 10 min. The reaction was stopped by placing the sample in a boiling water bath for 2 min. Each sample was then adjusted to pH 8.5 by the addition of 0.5 M of Tris-HCl (final concentration 50 mM) and incubated with 10 units of alkaline phosphatase (Roche Applied Science, from calf intestine) for 2 h, and the amount of dC was analyzed by the method of Steeper and Steuart (34) as revised in Ref. 35.

For activity determination of the reconstituted recombinant ββ′, a typical reaction mixture of 160 μl contained 50 mM HEPES, pH 7.5, 15 mM $MgSO_4$, 1 mM EDTA, 3 mM ATP, 50 mM DTT, 5 μM α_2, 1 μM ββ′, and 1 mM [5-^{3}H]CDP (4000–8000 cpm/nmol). Aliquots (50 μl) were removed at 0, 5, and 10 min and analyzed as described above.

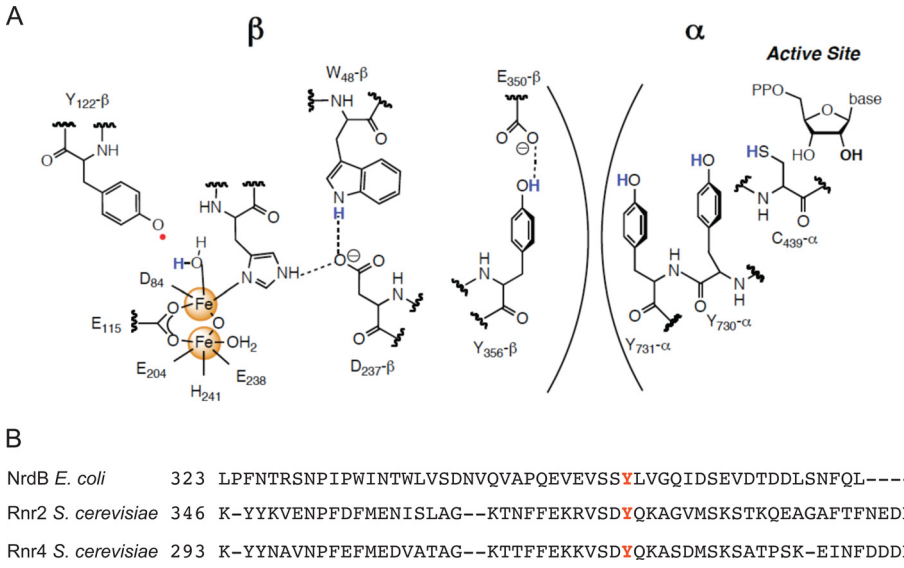

FIGURE 1. **The proposed long range RT pathway involves a conserved tyrosine residue in the C-terminal tail of class Ia RNR small subunit.** *A*, the proposed long range RT pathway between the α_2 and β_2 subunits (only one α and one β are shown) of the *E. coli* class Ia RNR. An essential tyrosine in the RT pathway, Tyr^{356} in *E. coli*, corresponds to Tyr^{376} and Tyr^{323} in β and β', respectively. *B*, sequence alignment of the C-terminal tails of the RNR small subunits from *E. coli* (NrdB) and *S. cerevisiae* (Rnr2(β) and RNR4(β')).

Western Blotting for β Protein Levels in Yeast Cell Extracts—Yeast cells (2×10^7) from log-phase cultures were treated with 200 μl of 0.1 M NaOH for 5 min at room temperature (36). The cells were pelleted by a brief centrifugation, resuspended in 200 μl of SDS loading buffer, and lysed by boiling in a sand bath for 5 min. Lysate from 1×10^6 cells (10 μl) was resolved by 10% SDS-PAGE, and the proteins were transferred to nitrocellulose membranes and probed with primary and secondary antibodies. The dilutions for antibodies were: polyclonal anti-β (31) at 1:200,000, monoclonal anti-Myc 9E10 (Covance) at 1:1,000, and goat-anti-mouse and goat-anti-rabbit (Jackson ImmunoResearch Laboratories) at 1:10,000. Blots were developed by using SuperSignal West Femto maximum sensitivity substrate (Thermo Scientific). A CCD camera (ChemiDoc XRS Bio-Rad) was used to record the blotting signals. The proteins were quantified by analyses of the signal intensities with Quantity One (Bio-Rad).

RESULTS

The C-terminal Tail of β′ Is Dispensable for Fe_2^{III}-Y• Formation in β—We have previously proposed that β' might use the aspartate and glutamate residues within its C-terminal tail (Figs. 1*B* and Fig. 2) to bind and deliver Fe^{II} to β in the $\beta\beta'$ heterodimer in a manner similar to that of copper loading of Sod1 by the chaperone protein Ccs1 (38, 39). To test this hypothesis, we previously constructed the β'-Δ8aa mutant that lacks the last 8 amino acid residues of β' (18). *In vitro* cluster assembly experiments using apo $\beta\beta'$ and $\beta\beta'$-Δ8aa, Fe^{2+}, and O_2 gave the same levels of Y•/$\beta\beta'$, suggesting that the tail did not play an essential role in this process. However, in contrast to the self-assembly studies in *E. coli* and mouse β_2, the yield of active yeast $\beta\beta'$ is poor (18). Thus, we have used the same constructs (18) to introduce β'_2 into permeabilized Δ*rnr4* cells that contain very low activity (<1% of WT), high levels of β_2, and undetectable Y• determined by whole cell EPR analysis (28). The addition of β'_2 to permeabilized Δ*rnr4* cells resulted in rapid heterodimer formation and Fe_2^{III}-Y• formation within 3 min (Fig. 3*A*, reproduced from supplemental Fig. 2*B* in Ref. 28). The $(\beta'\Delta 8aa)_2$ mutant gave the same amount of Fe_2^{III}-Y• as β'_2, suggesting that inside the cell, the β' C-terminal tail is not involved in iron delivery and cofactor formation.

The C-terminal Tail of β′ Is Essential for RNR Enzyme Activity, Indicating a Role in Interaction with α_2—In the experiments described above, the permeabilized Δ*rnr4* cells, subsequent to treatment with β'_2 for 10–20 s, were then incubated with 4.4 μM α_2 and 1 mM [^{3}H] CDP to assay for $\beta\beta'$ activity. Deoxy-CDP was produced at 3 nmol min^{-1} per A_{600} cells (Fig. 3*B*, *filled squares*). In contrast, with β'_2-Δ8aa under otherwise identical conditions, the activity was <0.5% of that of the WT β'_2 (Fig. 3*B*, *open squares*). Thus, although the C-terminal tail of β'_2 is dispensable for iron delivery and subsequent Fe_2^{III}-Y• assembly in β, it plays a crucial role in nucleotide reduction within the active holo-enzyme. The results indicate that an active complex is not formed at the concentrations of $(\beta'\Delta 8aa)_2$ (~6.5 μM) examined. Our previous studies have established that endogenous concentrations of β and β' in WT cells are 0.5–1.0 μM and that concentration of β in Δ*rnr4* cells is 5–10 μM (24). Thus, the C-terminal 8 amino acids of β' are critical for association with α_2 and formation of holo-enzyme.

Distinct Effects of Mutations of the E. coli NrdB Tyr^{356} Counterparts in β and β′ on Yeast Viability—Tyr^{356} (Tyr^{376} and Tyr^{323} in β and β', respectively, in *S. cerevisiae*, Figs. 1*B* and Fig. 2) within the C-terminal tail of the small subunit is conserved in all class I RNRs. One proposed function for this residue is its involvement in the delivery of the required reducing equivalent for assembly and maintenance of the Fe_2^{III}-Y• cofactor (20, 40). A second proposed function, established in the *E. coli* Ia RNR, is its involvement in the pathway of RT that is essential for nucleotide reduction (14, 15, 41, 42) (Fig. 1*A*).

To determine the functional importance of this tyrosine residue in β or β', we constructed *rnr2(Y376F)* and *rnr4(Y323F)*

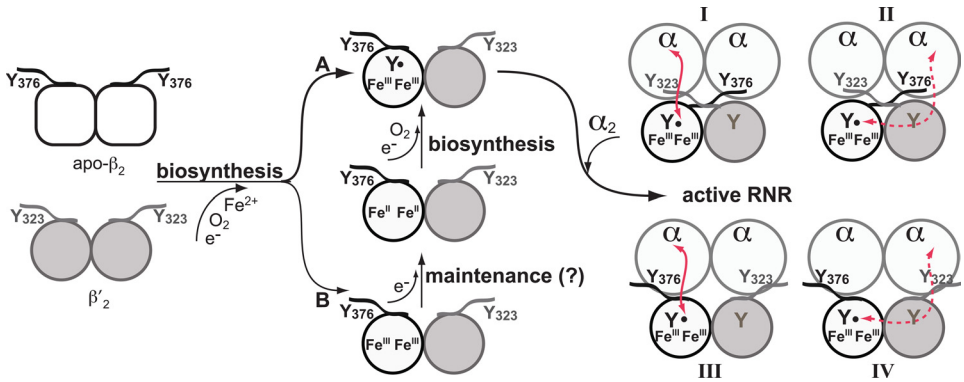

FIGURE 2. **Models depicting the roles of β and β′ C-terminal tails containing the conserved tyrosine residue (β-Tyr^{376} and β′-Tyr^{323}) in cluster biosynthesis/maintenance and association between ββ′ and α_2 to perform RT within the RNR holoenzyme.** Biosynthesis of the Fe^{III}_2-Y$^{\bullet}$ cofactor in ββ′ involves delivery of two Fe^{II} ions into β that in the presence of O_2 and a reducing equivalent provide an active $Fe^{III}Fe^{IV}$ species, which oxidizes β-Tyr^{183} in ββ′ to the Tyr$^{183\bullet}$ (*left panel*, *pathway A*). Cofactor can self-assemble *in vitro* when apo-$β_2$ and apo-$β'_2$ are mixed, which spontaneously form a heterodimer that then binds Fe^{II} and self-assembles with O_2 and reductant. Substoichiometric Y$^{\bullet}$/ββ′ levels with stoichiometric Fe^{III}_2 clusters are obtained both from *in vitro* self-assembly and from ββ′ isolated from yeast cells, indicating that some ββ′ is in an inactive Fe^{III}_2 (met) state (*left panel*, *pathway B*). Conversion of the Fe^{III}_2 to active cofactor can occur by a maintenance pathway that requires a reductant to generate the Fe^{II}_2 state, which can then assemble to form Fe^{III}_2-Y$^{\bullet}$ (*middle panel*). The conserved tyrosine residues at the C-terminal tails, β-Tyr^{376} and β′-Tyr^{323}, have been proposed to be involved in Fe^{II} delivery, in electron transfer required for cofactor biosynthesis and maintenance, and in RT between β and α to generate a thiyl radical in α. The C-terminal tails of β and β′ could cross over to interact with the distant α of the neighboring αβ pair (*right panel*, *I* and *II*) or interact exclusively with the proximal α of the same αβ pair (*right panel*, *III* and *IV*). *Red lines* indicate the putative RT pathway between α and β, which can occur between proximal (*I* and *III*) or distant (*II* and *IV*) α β subunits. The latter case requires a RT pathway across the ββ′ interface. Only model III is supported by experimental results in this study.

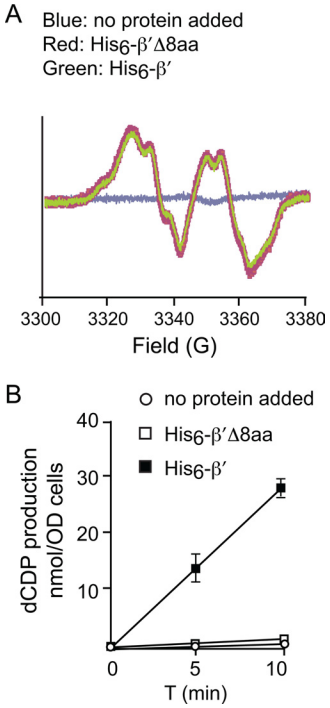

FIGURE 3. **Reconstitution of the Fe^{III}_2-Y$^{\bullet}$ cluster and RNR activity in permeabilized Δ*rnr4* cells by the addition of recombinant β′ and β′Δ8aa.** *A*, EPR analyses of permeabilized Δ*rnr4* cells in the presence of exogenous His_6-β′ (*green*), His_6-β′Δ8aa (*red*), or no protein addition (*blue*). *B*, specific activities of ββ′ were assayed using permeabilized Δ*rnr4* cells in the presence of exogenous His_6-β′ (*filled squares*) and α, His_6-β′Δ8aa (*open squares*) and α, or without any added protein (*open circles*).

mutant-containing plasmids and transformed them into the *RNR2* and *RNR4* shuffle strains, respectively. Each shuffle strain contains a chromosomal deletion of the gene being tested and is kept alive by a WT copy of the cognate gene on an *URA3*-marked plasmid. Survival of the transformants on media containing 5-fluoroorotic acid (5-FOA), a reagent that is converted by the *URA3* gene product to the cytotoxic chemical 5-fluorouracil that kills the Ura$^+$ cells, indicates that the mutant-bearing plasmids can provide the essential function in the absence of the WT copy on the *URA3* plasmid. The *rnr2(Y376F)* mutant failed to grow on a 5-FOA-containing plate (Fig. 4*A*). Western blotting confirmed the expression of the *rnr2(Y376F)* protein in the shuffle strain transformant prior to 5-FOA selection (Fig. 4*B*), indicating that the mutant protein was expressed but failed to replace the WT protein function. In contrast, the *rnr4(Y323F)* mutant was viable and exhibited no obvious difference in growth from the WT control strain on a 5-FOA plate (Fig. 4*C*). These results are consistent with the proposed essential role of β-Tyr^{376} either in Fe^{III}_2-Y$^{\bullet}$ assembly/maintenance or in the RT pathway, or both, and also indicate that β′-Tyr^{323} is not required for either event.

Measurement of in Vitro Fe^{III}_2-Y$^{\bullet}$ Cofactor Formation and Enzyme Activity of the C-terminal Tail Tyrosine Mutants of ββ′—Vegetative growth of yeast cells bearing the β(Y376F) and β′(Y323F) mutants offers a qualitative rather than quantitative measurement of their *in vivo* activity as the threshold of RNR activity to maintain viability or optimal growth in different yeast strains may vary. For instance, the Δ*rnr4* mutation is lethal in the W303 background (26) but viable in the S288C background despite very low Y$^{\bullet}$ content (not detectable by whole cell EPR) (28, 29). To gain mechanistic insight into the lethality resulting from the β(Y376F) mutant and to further rule out a role of β′-Tyr^{323} in RT, we have directly monitored *in vitro* the Fe^{III}_2-Y$^{\bullet}$ cluster assembly and activity of the ββ′ complexes formed from WT β, β′, and the β(Y376F) and β′(Y323F) mutants.

N-terminally His_6-tagged $β_2$, $β'_2$, $β_2$(Y376F), and $β'_2$(Y323F) were expressed in *E. coli*, purified to >95% homogeneity, and subjected to complex formation and cofactor reconstitution in four different combinations: ββ′, ββ′(Y323F), β(Y376F)β′, and β(Y376F)β′(Y323F) as described under "Experimental Procedures." EPR analyses of the resulting products show Y$^{\bullet}$ formation in all four experiments (Fig. 5*A*). Spin quantitation gave

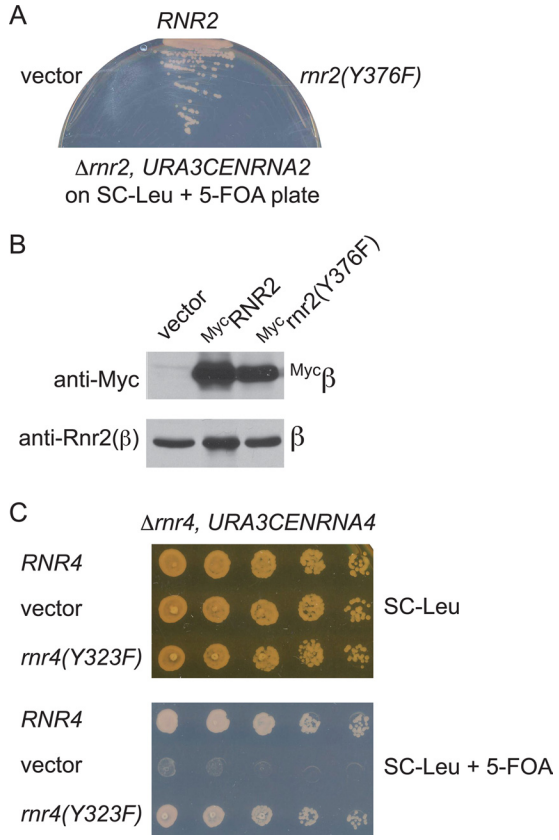

FIGURE 4. **Comparison of growth phenotypes of β(Y376F) and β′(Y323F) mutants lacking the conserved tyrosine residue in their C-terminal tails.** *A*, the β-Tyr^{376} residue is required for mitotic growth. *RNR2* shuffle strains (Δ*rnr2*, *URA3CENRNR2*) harboring a *CENLEU2* vector expressing WT-*RNR2* or the *rnr2(Y376F)* mutant were streaked onto a SC-Leu plate containing 5-FOA to eject the *URA3* plasmid. Growth on the 5-FOA plate indicates that the copy of *RNR2* on the *CENLEU2* plasmid can provide the essential *RNR2* function for mitotic survival. *B*, Western blots show comparable levels of the wild-type ^{Myc}Rnr2 and ^{Myc}Rnr2(Y376F) mutant proteins expressed in the *RNR2* shuffle strain before 5-FOA selection. *C*, the β′-Tyr^{323} is not required for mitotic growth. Serial dilutions (1:10, starting from 1×10^6 cells) of the *RNR4* shuffle strain (Δ*rnr4*, *URA3CENRNR4*) harboring a *CENHIS3* vector expressing the wild-type *RNR4* or the *rnr4(Y323F)* mutant were plated on a SC-His plate containing 5-FOA to eject the *URA3* plasmid. The plate was photographed after 3 days of incubation at 30 °C.

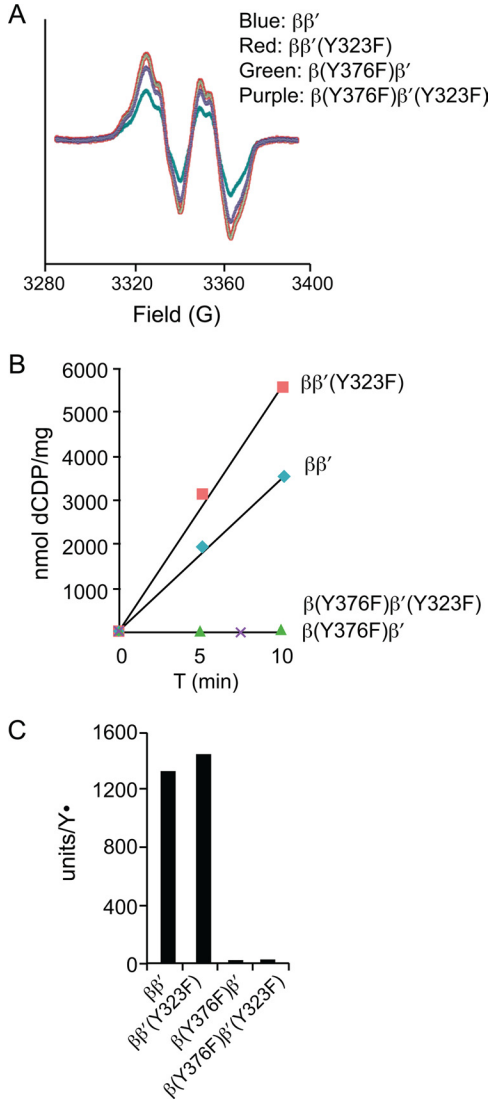

FIGURE 5. ***In vitro* reconstitution of the Fe_2^{III}-Y• cluster with purified recombinant wild-type and mutant β and β′ proteins.** *A*, EPR analyses of 20 μM reconstituted ββ′ complex from WT β with WT β′ (*blue*), WT β with β′(Y323F) (*red*), β(Y376F) with WT β′ (*green*), and β-Y376F with β′(Y323F) (*purple*). *B*, enzyme activity assays of reconstituted WT and mutant ββ′ complexes using radioactive CDP as a substrate in the presence of an excess of α_2. *C*, specific activities of WT and mutant ββ′ complexes normalized by Y• content.

0.25 Y• in WT ββ′ and ranged from 0.35 to 0.43 Y• with the mutant combinations. Thus, neither β-Tyr^{376} nor β′-Tyr^{323} is required for cofactor assembly *in vitro*. These reconstituted small subunits were then used to evaluate whether the C-terminal tyrosine residue is directly involved in the RT pathway by enzyme activity assays in the presence of an excess of α_2. Both ββ′ and ββ′(Y323F) were capable of converting CDP to dCDP, with specific activities proportional to the Y• contents (Fig. 4, *B* and *C*). By contrast, neither β(Y376F)β′ nor β(Y376F)β′(Y323F) exhibited any detectable catalytic activity despite comparable Y• levels in ββ′ and ββ′(Y323F) (Fig. 5, *B* and 5*C*). These results demonstrate that β-Tyr^{376} plays an essential role in the RT pathway, whereas β′-Tyr^{323} is dispensable in this process.

The β-Tyr^{376} Residue Is Not Required for Fe_2^{III}-Y• Cluster Formation in Vivo, Ruling out a Role in Electron Delivery in Cofactor—The β(Y376F) mutant is catalytically inactive and cannot support mitotic growth of yeast cells, although it is capable of forming the Fe_2^{III}-Y• cofactor *in vitro*. The self-assembly of the cofactor *in vitro* requires Fe^{2+} and O_2 with the reducing equivalent supplied by the Fe^{2+}. *In vivo*, we have proposed that this reducing equivalent is supplied by YfaE, a 2Fe2S cluster ferredoxin in *E. coli* (40, 43), and Dre2, an FeS requiring protein in *S. cerevisiae* (28). We wanted to test the proposal that β-Tyr^{376} is part of the electron transfer pathway to deliver the reducing equivalent for cluster assembly inside the cell. Because cells harboring β(Y376F) as the only source of β are unviable, we chose to examine a *GalRNR2* strain in which β expression from the chromosomal *RNR2* locus is controlled by the *GAL1* promoter. The *GalRNR2* cells propagate normally in galactose-containing media (*GAL* induced state) but are unable to grow in glucose-containing media (*GAL* repressed). When the trisaccharide raffinose is used as the sole carbon source for yeast cells, the *GAL* promoter is neither induced nor repressed, allowing basal levels of transcription (*i.e. GAL* uninduced or derepressed

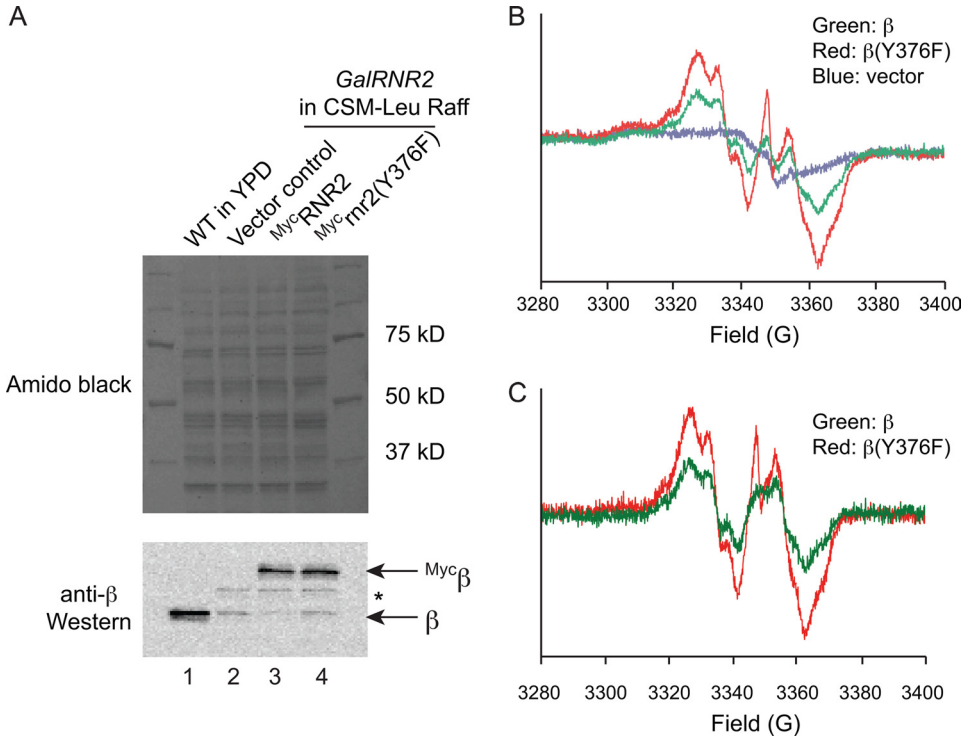

FIGURE 6. **Residue β-Tyr^{376} is not required for Fe_2^{III}-Y$^{\bullet}$ cluster formation *in vivo*.** *A*, Western blot showing comparable levels of ectopically expressed wild-type $^{Myc}\beta$ and $^{Myc}\beta$(Y376F) mutant proteins in the *GalRNR2* strain. Cells were inoculated from a CSM-Leu-Raff/Gal plate to 100 ml of CSM-Leu-Raff liquid medium and grown to a density of A_{600} ~1 over 16–20 h before being harvested, which depleted the endogenous, untagged β expressed from chromosomal *RNR2* locus. 1×10^6 cells were used for Western blotting, and the rest of cells (2×10^9) were used for EPR. Amido Black staining of the nitrocellulose membrane prior to Western blot shows equal loading of cell lysate (*upper* panel); Western blot using anti-β antibody detects both the untagged and 3×Myc-tagged β proteins (*lower panel*). *Lane 2* contains protein extracts from an untagged wild-type strain showing β expression level from the native *RNR2* promoter. The band between $^{Myc}\beta$ and β (marked by *) is a cross-reacting protein. *B*, whole cell EPR spectra of the *GalRNR2* cells harboring the empty vector (*blue*), $^{Myc}\beta$ (*green*), and $^{Myc}\beta$(Y376F) (*red*) in the *GalRNR2* cells grown in a raffinose-containing medium. *C*, EPR spectra after subtraction of the spectrum of vector control (*blue* in *B*) from $^{Myc}\beta$ (*green*) and $^{Myc}\beta$(Y376F) (*red*).

state). Consistent with low *GAL* promoter activity, *GalRNR2* cells cultured in raffinose media grow slowly with very low levels of endogenous β protein (Fig. 6*A*, *lanes 2–4*) and Y$^{\bullet}$ radical content (Fig. 6*B*, *blue*).

To study cluster assembly in β-mutants, we then transformed *CENLEU2* (low copy number, 1–3 copies/cell) (37) plasmids with the ability to express N-terminally Myc-tagged β WT and β(Y376F) from the native *RNR2* promoter into the *GalRNR2* cells. *GalRNR2* transformants harboring the empty *CENLEU2* vector were used as a negative control. All sets of transformants were inoculated from CSM-Leu-Raff/Gal plate (*GAL* induced) to 100 of ml CSM-Leu-Raff liquid medium (*GAL* uninduced) and grown to a density of A_{600} ~1 over 16–20 h. At this time, the endogenous, untagged β expressed from *GalRNR2* was depleted to residual levels (Fig. 6*A*, *lanes 2–4*), and the ectopically expressed Myc-β and Myc-β(Y376F) are present at levels that are 7–14-fold higher (Fig. 6*A*, *lanes 3* and *4*). These levels are comparable with that of the endogenous β in a WT control strain (Fig. 6*A*, compare *lane 1* with *lanes 3* and *4*). The moderately (~60%) higher level of Myc-β(Y376F) is likely due to mild checkpoint activation resulting from the absence of a functional β.

The elevated levels of ectopically expressed Myc-β and Myc-β(Y376F) over the endogenous β under the experimental conditions allowed us to determine and compare Fe_2^{III}-Y$^{\bullet}$ cluster content between the two strains using whole cell EPR spectroscopy (Fig. 6*B*). The Y$^{\bullet}$ was detectable in both the Myc-β-expressing cells (*green*) and the Myc-β(Y376F)-expressing cells (*red*) but was not detectable in cells carrying the control vector (*blue*).

The EPR spectrum from the vector control was used as a background signal and was subtracted from both the Myc-β and the Myc-β(Y376F) samples. The analysis shown in Fig. 5*C* revealed that Myc-β(Y376F)-expressing cells have a Y$^{\bullet}$ content that is 60% higher than that from the Myc-β-expressing cells. When the Y$^{\bullet}$ signals were normalized for levels of the Myc-β and Myc-β(Y376F) proteins, respectively (Fig. 6*A*), there was no difference in steady-state Fe_2^{III}-Y$^{\bullet}$ cluster content between wild-type β and the β(Y376F) mutant. The results together demonstrate that β-Tyr^{376} is not required for Fe_2^{III}-Y$^{\bullet}$ cluster formation *in vivo*. It should be noted, however, that the *in vivo* rates of cluster assembly cannot be analyzed under the experimental conditions.

DISCUSSION

In this study, we provide evidence that the C-terminal tail of β′ does not cross over to the neighboring αβ pair thus providing, insights into the geometry of ββ′ C-terminal tails relative to α_2 within the holoenzyme. The unusual heterodimeric structure of yeast small subunit ββ′ with only a single Fe_2^{III}-Y$^{\bullet}$ cluster per ββ′ have provided a unique system to investigate the RT pathway and the quaternary structure of the RNR holoenzyme

in an active complex inside the cell. Although β′ on its own does not form a Fe_2^{III}-Y• cluster (18, 24, 26, 31), it is conceivable that Tyr^{323} of β′ could participate in the RT process as a stepping stone between the α_2 and ββ′ during the turnover cycle (18). In this proposal, the C terminus of β′ would not interact with the α of its own α/β′ pair, but instead would interact with the α of the neighboring α/β pair, which contains the Fe_2^{III}-Y• cofactor. Thus, this proposal posits that the C-terminal tail of β′ would cross over at the subunit interface (Fig. 2, *right panel*, *I* and *II*). However, our observation that the β(Y376F) mutant is catalytically inactive and causes cell lethality, whereas the β′(Y323F) mutant has no effect on either yeast vegetative growth or enzyme activity, strongly suggests that the tails of β and β′ do not cross over to interact with the adjacent α within the holocomplex. Instead, each β and β′ tail interacts with the proximal α in the same α/β (α/β′) pair (Fig. 2, *right panel*, *III* and *IV*).

In the studies of Ge *et al.* (35) in 2003, single turnover experiments using the *E. coli* $\alpha_2\beta_2$ with one Y•/β_2 observed formation of two dCDPs with the same rate constant (35). At the time, two hypotheses were proposed for this unusual observation that a single Y• could service both active sites in α_2. One hypothesis was that in addition to the established RT pathway between the proximal α and β (Fig. 2, *right panel*, *I* and *III*), there was a second RT pathway involving both Trp^{48} and Tyr^{356} in β with the electron transfer occurring across the β-β monomer interface via the two Trp^{48} residues to generate a thiyl radical in the second α (Fig. 2, *right panel*, *II* and *IV*). A second hypothesis involved rapid dissociation of β_2 from α_2 and their subsequent rapid reassociation, both faster than turnover, to allow the second dCDP to be generated quickly in the second α of the α_2. Our results with the β(Y376F) and β′(Y323F) mutants suggest that the former hypothesis is unlikely for the yeast RNR. If RT could cross the β-β′ interface and generate thiyl radical in the active site of the adjacent α according to the first model, then the β-Y376F mutant would not have completely inactivated the enzyme as observed. Thus, our studies support the model in which RT occurs only within one α/β pair (Fig. 2, *right panel*, *III*).

In vitro reconstitution of the Fe_2^{III}-Y• cofactor uses excess ferrous iron to provide reducing equivalent required for its formation (11). However, *in vivo*, a ferredoxin-like protein YfaE in *E. coli* (43) and an FeS cluster-containing protein Dre2 (28) in *S. cerevisiae* have been proposed to provide electrons for the Fe_2^{III}-Y• formation and maintenance pathways. Before the identification of YfaE, Coves *et al.* (20) showed *in vitro* that a reduced met-β could regenerate the active Fe_2^{III}-Y•-containing β and that the C-terminal tail Tyr^{356} was important for this process (20). The C-terminal Tyr^{356} was proposed to mediate electron transfer for the maintenance of the cofactor and potentially for cofactor assembly. Our whole cell EPR results with the β(Y376F) mutant in the *GalRNR2* cells at uninduced state clearly demonstrate for the first time that β-Tyr^{376} is not required for Fe_2^{III}-Y• formation *in vivo*, and thus, its essential function is likely due to its role in the RT pathway.

REFERENCES

1. Nordlund, P., and Reichard, P. (2006) Ribonucleotide reductases. *Annu. Rev. Biochem.* **75,** 681–706
2. van der Donk, W. A., Yu, G., Pérez, L., Sanchez, R. J., Stubbe, J., Samano, V., and Robins, M. J. (1998) Detection of a new substrate-derived radical during inactivation of ribonucleotide reductase from *Escherichia coli* by gemcitabine 5′-diphosphate. *Biochemistry* **37,** 6419–6426
3. Ando, N., Brignole, E. J., Zimanyi, C. M., Funk, M. A., Yokoyama, K., Asturias, F. J., Stubbe, J., and Drennan, C. L. (2011) Structural interconversions modulate activity of *Escherichia coli* ribonucleotide reductase. *Proc. Natl. Acad. Sci. U.S.A.* **108,** 21046–21051
4. Minnihan, E. C., Ando, N., Brignole, E. J., Olshansky, L., Chittuluru, J., Asturias, F. J., Drennan, C. L., Nocera, D. G., and Stubbe, J. (2013) Generation of a stable, aminotyrosyl radical-induced α2β2 complex of *Escherichia coli* class Ia ribonucleotide reductase. *Proc. Natl. Acad. Sci. U.S.A.* **110,** 3835–3840
5. Rofougaran, R., Vodnala, M., and Hofer, A. (2006) Enzymatically active mammalian ribonucleotide reductase exists primarily as an α6β2 octamer. *J. Biol. Chem.* **281,** 27705–27711
6. Wang, J., Lohman, G. J., and Stubbe, J. (2009) Mechanism of inactivation of human ribonucleotide reductase with p53R2 by gemcitabine 5′-diphosphate. *Biochemistry* **48,** 11612–11621
7. Rofougaran, R., Crona, M., Vodnala, M., Sjöberg, B. M., and Hofer, A. (2008) Oligomerization status directs overall activity regulation of the *Escherichia coli* class Ia ribonucleotide reductase. *J. Biol. Chem.* **283,** 35310–35318
8. Fairman, J. W., Wijerathna, S. R., Ahmad, M. F., Xu, H., Nakano, R., Jha, S., Prendergast, J., Welin, R. M., Flodin, S., Roos, A., Nordlund, P., Li, Z., Walz, T., and Dealwis, C. G. (2011) Structural basis for allosteric regulation of human ribonucleotide reductase by nucleotide-induced oligomerization. *Nat. Struct. Mol. Biol.* **18,** 316–322
9. Kashlan, O. B., and Cooperman, B. S. (2003) Comprehensive model for allosteric regulation of mammalian ribonucleotide reductase: refinements and consequences. *Biochemistry* **42,** 1696–1706
10. Hofer, A., Crona, M., Logan, D. T., and Sjöberg, B. M. (2012) DNA building blocks: keeping control of manufacture. *Crit. Rev. Biochem. Mol. Biol.* **47,** 50–63
11. Cotruvo, J. A., and Stubbe, J. (2011) Class I ribonucleotide reductases: metallocofactor assembly and repair *in vitro* and *in vivo*. *Annu. Rev. Biochem.* **80,** 733–767
12. Uhlin, U., and Eklund, H. (1994) Structure of ribonucleotide reductase protein R1. *Nature* **370,** 533–539
13. Nordlund, P., Sjöberg, B. M., and Eklund, H. (1990) Three-dimensional structure of the free radical protein of ribonucleotide reductase. *Nature* **345,** 593–598
14. Climent, I., Sjöberg, B. M., and Huang, C. Y. (1991) Carboxyl-terminal peptides as probes for *Escherichia coli* ribonucleotide reductase subunit interaction: kinetic analysis of inhibition studies. *Biochemistry* **30,** 5164–5171
15. Climent, I., Sjöberg, B. M., and Huang, C. Y. (1992) Site-directed mutagenesis and deletion of the carboxyl terminus of *Escherichia coli* ribonucleotide reductase protein R2. Effects on catalytic activity and subunit interaction. *Biochemistry* **31,** 4801–4807
16. Cohen, E. A., Gaudreau, P., Brazeau, P., and Langelier, Y. (1986) Specific inhibition of herpesvirus ribonucleotide reductase by a nonapeptide derived from the carboxy terminus of subunit 2. *Nature* **321,** 441–443
17. Dutia, B. M., Frame, M. C., Subak-Sharpe, J. H., Clark, W. N., and Marsden, H. S. (1986) Specific inhibition of herpesvirus ribonucleotide reductase by synthetic peptides. *Nature* **321,** 439–441
18. Ge, J., Perlstein, D. L., Nguyen, H. H., Bar, G., Griffin, R. G., and Stubbe, J. (2001) Why multiple small subunits (Y2 and Y4) for yeast ribonucleotide reductase? Toward understanding the role of Y4. *Proc. Natl. Acad. Sci. U.S.A.* **98,** 10067–10072
19. Eklund, H., Uhlin, U., Färnegårdh, M., Logan, D. T., and Nordlund, P. (2001) Structure and function of the radical enzyme ribonucleotide reductase. *Prog. Biophys. Mol. Biol.* **77,** 177–268
20. Covès, J., Delon, B., Climent, I., Sjöberg, B. M., and Fontecave, M. (1995) Enzymic and chemical reduction of the iron center of the *Escherichia coli* ribonucleotide reductase protein R2. The role of the C-terminus. *Eur. J. Biochem.* **233,** 357–363
21. Minnihan, C. C., Nocera, D. G., and Stubbe, J. (2013) Reversible long-

range radical transfer in class Ia ribonucleotide reductase. *Acc. Chem. Res.*, in press
22. Chabes, A., Domkin, V., Larsson, G., Liu, A., Gräslund, A., Wijmenga, S., and Thelander, L. (2000) Yeast ribonucleotide reductase has a heterodimeric iron-radical-containing subunit. *Proc. Natl. Acad. Sci. U.S.A.* **97,** 2474–2479
23. Sommerhalter, M., Voegtli, W. C., Perlstein, D. L., Ge, J., Stubbe, J., and Rosenzweig, A. C. (2004) Structures of the yeast ribonucleotide reductase Rnr2 and Rnr4 homodimers. *Biochemistry* **43,** 7736–7742
24. Perlstein, D. L., Ge, J., Ortigosa, A. D., Robblee, J. H., Zhang, Z., Huang, M., and Stubbe, J. (2005) The active form of the *Saccharomyces cerevisiae* ribonucleotide reductase small subunit is a heterodimer *in vitro* and *in vivo*. *Biochemistry* **44,** 15366–15377
25. An, X., Zhang, Z., Yang, K., and Huang, M. (2006) Cotransport of the heterodimeric small subunit of the *Saccharomyces cerevisiae* ribonucleotide reductase between the nucleus and the cytoplasm. *Genetics* **173,** 63–73
26. Huang, M., and Elledge, S. J. (1997) Identification of RNR4, encoding a second essential small subunit of ribonucleotide reductase in *Saccharomyces cerevisiae*. *Mol. Cell. Biol.* **17,** 6105–6113
27. Wang, P. J., Chabes, A., Casagrande, R., Tian, X. C., Thelander, L., and Huffaker, T. C. (1997) Rnr4p, a novel ribonucleotide reductase small-subunit protein. *Mol. Cell. Biol.* **17,** 6114–6121
28. Zhang, Y., Liu, L., Wu, X., An, X., Stubbe, J., and Huang, M. (2011) Investigation of *in vivo* diferric tyrosyl radical formation in *Saccharomyces cerevisiae* Rnr2 protein: requirement of Rnr4 and contribution of Grx3/4 AND Dre2 proteins. *J. Biol. Chem.* **286,** 41499–41509
29. Ortigosa, A. D., Hristova, D., Perlstein, D. L., Zhang, Z., Huang, M., and Stubbe, J. (2006) Determination of the *in vivo* stoichiometry of tyrosyl radical per $\beta\beta'$ in *Saccharomyces cerevisiae* ribonucleotide reductase. *Biochemistry* **45,** 12282–12294
30. Longtine, M. S., McKenzie, A., 3rd, Demarini, D. J., Shah, N. G., Wach, A., Brachat, A., Philippsen, P., and Pringle, J. R. (1998) Additional modules for versatile and economical PCR-based gene deletion and modification in *Saccharomyces cerevisiae*. *Yeast* **14,** 953–961
31. Nguyen, H. H., Ge, J., Perlstein, D. L., and Stubbe, J. (1999) Purification of ribonucleotide reductase subunits Y1, Y2, Y3, and Y4 from yeast: Y4 plays a key role in diiron cluster assembly. *Proc. Natl. Acad. Sci. U.S.A.* **96,** 12339–12344
32. Atkin, C. L., Thelander, L., Reichard, P., and Lang, G. (1973) Iron and free radical in ribonucleotide reductase. Exchange of iron and Mossbauer spectroscopy of the protein B2 subunit of the *Escherichia coli* enzyme. *J. Biol. Chem.* **248,** 7464–7472
33. Bollinger, J. M., Jr., Tong, W. H., Ravi, N., Huynh, B. H., Edmondson, D. E., and Stubbe, J. (1995) Use of rapid kinetics methods to study the assembly of the diferric-tyrosyl radical cofactor of *Escherichia coli* ribonucleotide reductase. *Methods Enzymol.* **258,** 278–303
34. Steeper, J. R., and Steuart, C. D. (1970) A rapid assay for CDP reductase activity in mammalian cell extracts. *Anal. Biochem.* **34,** 123–130
35. Ge, J., Yu, G., Ator, M. A., and Stubbe, J. (2003) Pre-steady-state and steady-state kinetic analysis of *E. coli* class I ribonucleotide reductase. *Biochemistry* **42,** 10071–10083
36. Kushnirov, V. V. (2000) Rapid and reliable protein extraction from yeast. *Yeast* **16,** 857–860
37. Koshland, D., Kent, J. C., and Hartwell, L. H. (1985) Genetic analysis of the mitotic transmission of minichromosomes. *Cell.* **40,** 393–403
38. Culotta, V. C., Klomp, L. W., Strain, J., Casareno, R. L., Krems, B., and Gitlin, J. D. (1997) The copper chaperone for superoxide dismutase. *J. Biol. Chem.* **272,** 23469–23472
39. Lamb, A. L., Torres, A. S., O'Halloran, T. V., and Rosenzweig, A. C. (2001) Heterodimeric structure of superoxide dismutase in complex with its metallochaperone. *Nat. Struct. Biol.* **8,** 751–755
40. Hristova, D., Wu, C. H., Jiang, W., Krebs, C., and Stubbe, J. (2008) Importance of the maintenance pathway in the regulation of the activity of *Escherichia coli* ribonucleotide reductase. *Biochemistry* **47,** 3989–3999
41. Yee, C. S., Chang, M. C., Ge, J., Nocera, D. G., and Stubbe, J. (2003) 2,3-difluorotyrosine at position 356 of ribonucleotide reductase R2: a probe of long-range proton-coupled electron transfer. *J. Am. Chem. Soc.* **125,** 10506–10507
42. Yee, C. S., Seyedsayamdost, M. R., Chang, M. C., Nocera, D. G., and Stubbe, J. (2003) Generation of the R2 subunit of ribonucleotide reductase by intein chemistry: insertion of 3-nitrotyrosine at residue 356 as a probe of the radical initiation process. *Biochemistry* **42,** 14541–14552
43. Wu, C.-H., Jiang, W., Krebs, C., and Stubbe, J. (2007) YfaE, a ferredoxin involved in diferric-tyrosyl radical maintenance in *Escherichia coli* ribonucleotide reductase. *Biochemistry* **46,** 11577–11588